Off-peak and Window Width Shift of Energy Induced a False Diagnosis during Planer and SPECT Images

* Rizk AR, *Abdelhalim MAK, Hamed I F**, and Sameh R**
* Department of Physics, Faculty of Science, Helwan University, Egypt.
**Radiotherapy and Nuclear Medicine Department, National Cancer Institute, Cairo University, Egypt.

Abstract: To investigate the radiopharmaceutical distribution in one or more sections of some organs, single photon emission computed tomography technique (SPECT) was used, by which the camera detect the distribution of the injected radiopharmaceutical from varying angles around the patient body at fixed intervals. Thus, the gamma camera must work at some optimum conditions to avoid interpretation mistakes, which can be generated due to the protocol errors. One of these errors is the camera non-uniformity. Among the different factors affecting the camera uniformity were off-peak shift (off-peak %), which was defined as the shift of the specified isotope peak from its real position and window width shift of energy. In the present study, we investigated the effect of both of the off-peak shift and window width shift of energy on planer and SPECT image uniformity using a point source to perform flood images, and by plotting the relation between the calculated integral and differential center field of view (CFOV) and useful field of view (UFOV) uniformity values versus the change of both of the off-peak and window width shift. Moreover, we investigated the images of different flood phantom with both of the different off-peaks and window width shifts. We concluded that the optimum off-peak shift was 0% shift, but practically we can acquire data in the range of 0% to 2% off-peak shifts without deeply effect on the image quality. In SPECT study, the effect of off-peak shift and window width shift applied on heart phantom affected the quality of images strongly leading to different clinical diagnosis, and the optimum window width shift was in the range of 15% to 20% shift of energy for the used isotope. Finally, the application of off-peak and widow width shift of energy on patients during the thyroid and kidney scan have reported a high level of severity with a false diagnosis.

Keywords: radiopharmaceutical; nuclear imaging; SPECT; gamma camera; off-peak shift; window width shift.

Introduction: Nuclear Imaging technique is one of the most important tools for physicians to diagnose or to confirm a disease. Diagnostic imaging of lung, Brian, thyroid, heart, liver, etc. is achieved using sophisticated gamma camera, with topographic facilities linked to computer systems (4). The gamma camera was the most familiar imaging tool in nuclear medicine to obtain a good representative image, in which a patient is injected by a suitable radiopharmaceutical which emits gamma rays that can be detected from outside the body by a gamma camera. This would give information on the physiology and radiopharmaceutical distribution in the organ of interest. The gamma camera can be used for static and dynamic imaging as well as for SPECT imaging where several static images from different angles can be recorded to give images in three dimensions (11). It has been reported that SPECT significantly improved image contrast over planar imaging and has the ability to separate overlapping structures (6). Camera systems with 2 or more heads (multi-head systems) and with more detectors offered more optimal spatial resolution and sensitivity characteristics than those with a single-head system (12). Quality control performed on nuclear medicine cameras provided the confidence to technologists and physicians that a SPECT scan supplies an accurate representation of the radiopharmaceutical distribution in the patient. Graham 1995 has reported the quality control for SPECT systems. The SPECT corrections that have the most significant effects

on the reconstructed image quality were the uniformity correction (the ability of a gamma camera to reproduce a uniform radioactive distribution by using a uniform source and applying this correction to patient images) and center of rotation correction (adjust the mechanics and the software to rotate around a fixed center (6, 7, 8 and 10). The most sensitive indicator of gamma-camera performance is the uniformity (13). Most artifacts related to the integrity of the detector head, computer system, and hard copy device can be detected on the uniformity image. It has been reported that the best way to avoid artifacts is to pay very close attention to the technical factors of image acquisition and processing and to be aware of attenuation factors (3). Baron et al., 1996 have reported that nuclear medicine imaging had not reached the level of standardization, automation, because of the large number of parameters and other factors affecting the image uniformity. Agostini et al., 1987 have found that SPECT using a rotating gamma camera needs accurate calibration of electromechanical components, detection system and reconstruction software. O'Connor 1996 has reported that the advances in gamma-camera design over the last 5 to 10 years have improved most of the aspects of image quality, particularly for tomography imaging (9). Thus, the aim of the present study was to investigate the effect of off-peak shift and window width shift of energy on planer and SPECT image uniformity by studying the relation between both of the off peak shift and window width shift of energy, and the integral and deferential uniformity of both of the center field of view (CFOV) and useful field of view (UFOV) values to elucidate the role of both of the off-peak and window width shift of energy on the planer and SPECT image uniformity as well as to clarify and investigate their role in some clinical cases.

Materials and methods:

Gamma camera: Gamma camera used in the present study is a dual head variable angle system, model E. camera, manufactured by Siemens (USA), and installed in National Cancer Institute-Cairo, Egypt. It consists of gantry with detectors (includes remote hand control units and display panel mounted on the top of gantry), detectors, collimators, collimator servers, patient bed and acquisition controller.

Tc-99m generator: Technetium generator (Pharma Company Cited in Belgium) produces a sterile solution of Tc-99m as sodium pertechnetate. This solution is eluted using a 0.9% sterile and endotoxin free solution of sodium chloride from an alumina (AL_2O_3 chromatography column. The daughter Tc-99m is held chemically much less tightly than Mo-99 to the column material and the eluant, which consists of nearly pure sodium pertechnetate, is then ready for the combination with an agent to form the radiopharmaceutical.

Point source: A small ball of cotton to concentrate the radioactivity in a small and uniform size with Tc-99m activity between 20-30µCi are placed in a small plastic cone. The cone is used to get the smallest concentrated source and to avoid the scattering. Use a little liquid as possible and ensure that the point source is correct by measuring it in a dose calibrator (Model V-304, Supplied from Veenstra Instruments, Netherlands). Place a small piece of cotton (approximately 3 mm in diameter) into the vial; it should not fill the entire vial. Place drops of the desired activity of Technetium on the cotton, such that it does not exceed the cotton's saturation capacity, and then measure the activity of Tc-99 m.

Source set up for peaking, tuning, uniformity check and intrinsic flood: Remove the collimators, fully retract the detectors and rotate the gantry so detector 1 is at 0º and detector 2 at 180º. Extend the integrated source holder from its storage position in the rear bed and pull it until the source holder is approximately centered. Prepare the point source as described previously. Clamp the capped end of the vial into the source holder and ensure that the cotton tip with the activity is approximately centered above detector 2, and below detector 1, move the bed up and down until the source is centered between the two detectors. Check the displayed spectrum to ensure that you have a scattering-free source.

To peak the detector, slightly shift the analyzer's window so that it is centered on the energy peak. The detectors must be turned on, during whole peaking steps. Select the isotope being to peak and click on the peak bottom, the system peaks the activated detector(s) according to the analyzer values. When the peaking process is completed, it automatically enters the appropriate status in the peak status field. Off-peak shift % represents how far the system had to shift the detected isotope photo-peak, to make it to comply with the established analyzer values.

Uniformity calculation: The system updates the intrinsic correction data only if you collect at least 50 million counts. For SPECT studies in 64 x 64 or 128 x128 matrixes, floods of 50 million counts are sufficient to correct the images. Using the PPM, verify that the count rate is approximately the same at each detector. If the count rate between the detectors isn't within 5% of each other, adjust the pallet, and therefore the source. Keep adjusting the pallet position until the count rate between the detectors falls within the 5% range. The computer software of the gantry control is running under UNIX operating system. For the acquisition and image processing, the computer is running under Apple Macintosh. The system with the soft ware is designed by Siemens Company (Germany). Spatial image analysis software is used to calculate the integral and differential uniformity % of UFOV and CFOV. The non-uniformity measured from the counts stored in individual pixel values in the computer may be calculated as follows:

The integral uniformity (IU) %: IU (%) = 100 x (Max – Min) / (Max + Min), where: Max: is the maximum pixel count.
Min: s the minimum pixel count.

The differential uniformity (DU) %: DU (%) = 100 x (Hi –Low) / (Hi + Low), where: hi and low, are max and min pixel counts respectively, for all rows and columns within a localized line of pixels, in which hi-low is the largest deviation.

Preparation of the lung heart phantom: The outer cavity of heart phantom is filled with approximately 1.5 mCi Tc-99m, and then leaves a small residual air bubble. Fix the heart phantom inside the lung phantom, and then fill the lung phantom by water. Carefully place the cover plate on the phantom and tighten it down by gently applying pressure by hand to the plate and carefully screwing in the cover plate screws. Filling the phantom through the filler holes in the top cover plate, and then injects water into the phantom until the solution level nears to the cover plate by using syringe, now screw all the filler plugs and leave one. Tilt the phantom so that the remaining air bubbles move toward the open filler hole, steadily inject water into the open hole until the phantom is completely filled and lastly screw the final filler plug.

The effect of off peak and window width shift of energy on the image uniformity: The relation between the integral and differential center field of view (CFOV) and useful field of view (UFOV) uniformity values at different off-peak and widow width shift of energy values were investigated. It was done as follows: Set up the source as previously described. Open the analyzer to adjust the off peak and the window width shift of energy, in our case we change the off-peak by shifting the window width by 2%, 3%, 4%, 5%, and 6% keeping the same window width shift of energy, and then start an acquisition for acquiring intrinsic flood. Change the window width shift of energy from the analyzer, and then repeat the previous steps. Acquisition parameters are camera information, matrix size (256 x 256), magnification (1.0), window width shift of energy (10% 15% and 20%), count rate (50K cuts/sec), scan information and collected counts (50,000,000 counts).

Effect of off-peak and window width shift of energy on SPECT images uniformity using heart phantom: The heart phantom is used in multi SPECT acquisitions for different off-peaks and window width shifts using the same parameters in each acquisition. For this purpose, the heart lung phantom is prepared as before. Place the phantom on the patient bed as a patient, and fix all the acquisition parameters. Change only the off-peak shift of energy as 2%, 3%, 4%, 5% and 6%, and then repeat the previous step. Start an

acquisition of SPECT study, then change the window width shift of energy as 5%, 10%, 15%, 20% and 25%, and then repeat the previous steps. Acquisition parameters are camera information, matrix size (64 x64), magnification (1.45), window width (5%, 10%, 15%, 20% and 25%), count rate (50 K cuts/sec), scan information, rotation type, step and shoot, orbit type, body contour, number of views per scan 32 and detectors configuration (90^o).

Application of thyroid and renal scan: This scan is done on a patient injected 3 mCi Tc-99m, and then imaged after 20 minutes for 4 times by the same parameters each time with changing the off-peak shift of energy as 0%, 2%, 4% and 6%. Set up the patient on the bed with extended neck, open the analyzer and adjust the off-peak and the window width shift of energy. In this case we changed the off-peak shift of energy by shifting the window by 0%, 2%, 4% and 6% at the same window width, and then an acquisition for acquiring thyroid image is done. The off-peak shift from the analyzer is changed, and then the previous steps are repeated. Acquisition parameters are camera information, matrix size (256 x 256), magnification 3.2 for thyroid and 1 for renal, window width 15%, scan information and collected counts (700,000 counts).

Results and discussions

Fig. 1 represents the relative number of counts versus the photo-peak of Tc-99m at 140 keV and the widow width 20% width. Off-peak 0% means that the photo-peak of Tc-99m is at 140 keV as shown in Fig. 1.

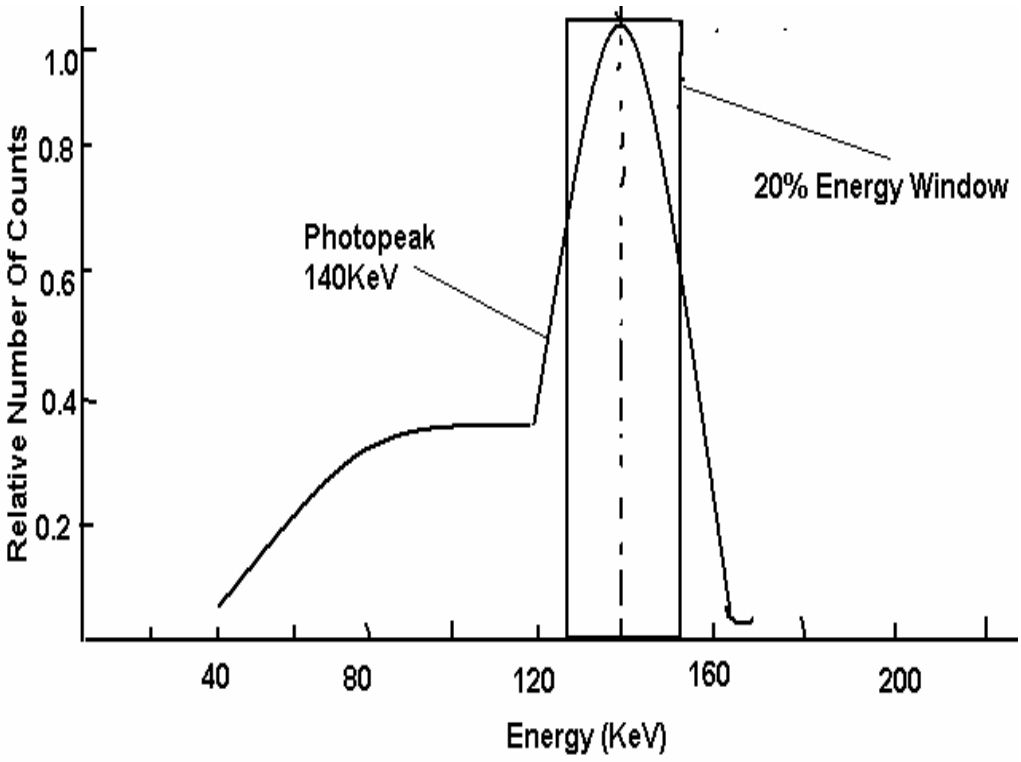

Fig. 1 A photo-peak of Tc-99m at 140 keV and window width 20%

The integral and differential in both center field of view (CFOV) and useful field of view (UFOV) uniformity values in arbitrary units for 0%, 2%, 3%, 4%, 5% and 6% off-peak shift of energy, at 10%, 15% and 20% window width, respectively are shown in Fig 2, 3 and 4. In Figs. 2, 3 and 4, no significant increase in the calculated values of uniformity at the off-peak 0% and 2% can be noted, which indicates a small loss of uniformity in that range. Whereas, in the off-peak% range of 2% to 6%, there is a significant change in the integral and differential values in both fields (CFOV and UFOV), which indicate an instability and significant change in uniformity in that range.

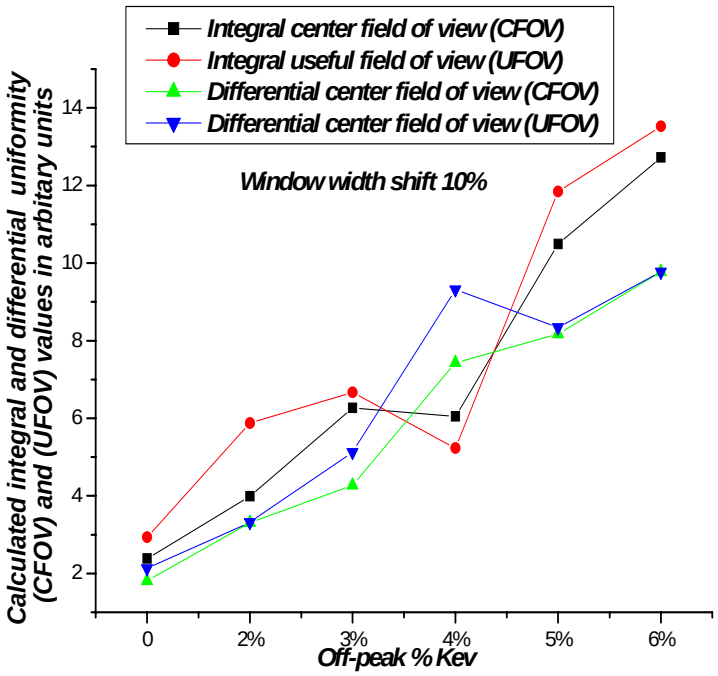

Fig. 2 represents the calculated integral and differential uniformity (CFOV) and (UFOV) values in arbitary units versus Off-peak% in KeV at window width shift 10%.

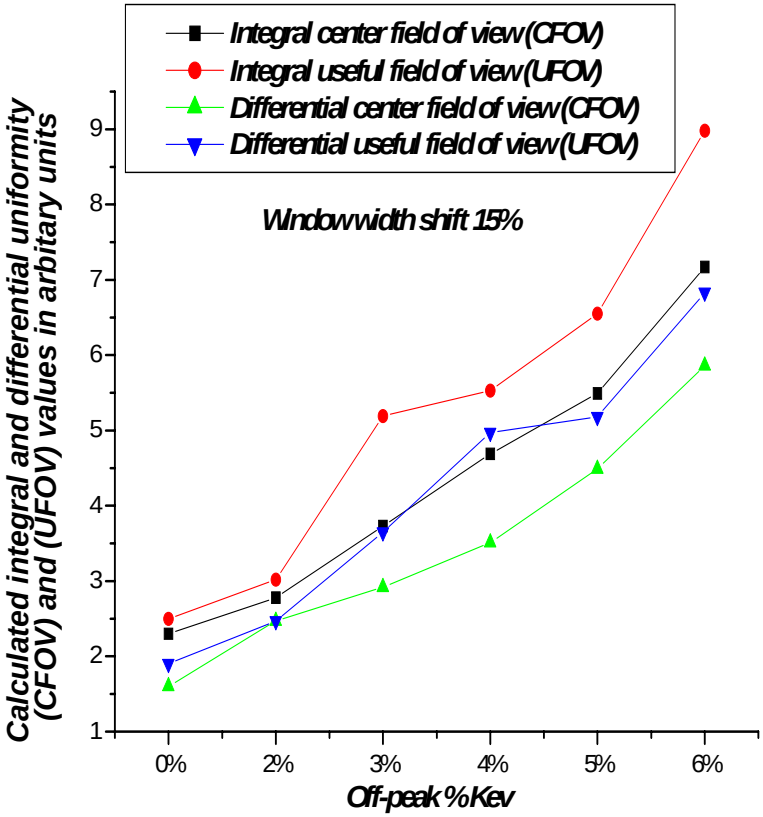

Fig. 3 represents the calculated integral and differential uniformity (CFOV) and (UFOV) values in arbitary units versus Off-peak% in Kev at window width shift 15%

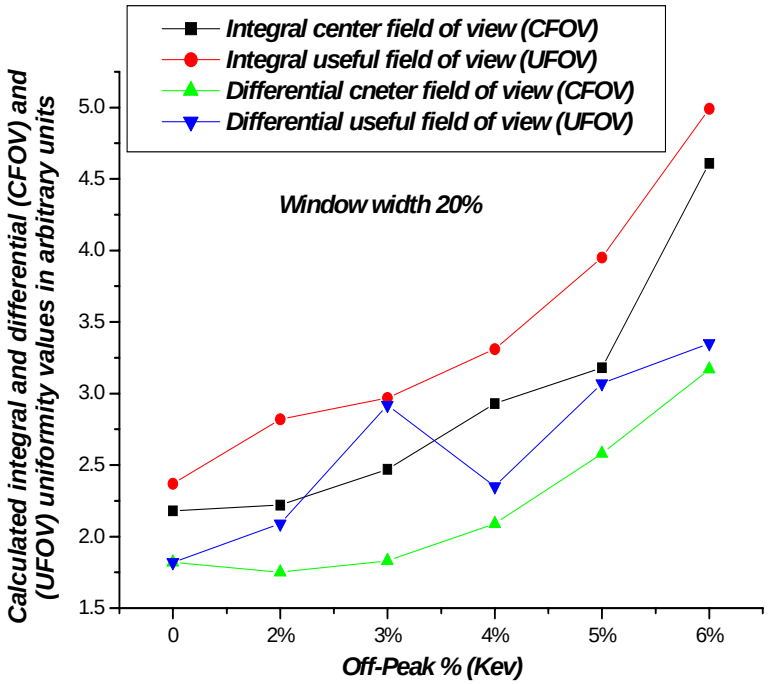

Fig. 4 represents the calculated integral and differential uniformity (CFOV) and (UFOV) values in arbitary units versus Off-peak% in KeV at window width 20%.

Figs. 5, 6 and 7 presents the images of flood for different uniformity values due to the change in the off-peak percentage, at window width of 10%, 15% and 20%, respectively. Hot and cold areas (dark and bright spots) which are shown in the images of these Figs. 5, 6 and 7 offer good evidence on the decrease in uniformity with increasing the off-peak percentage. Moreover, the distinguishably between hot and cold areas are not clearly visualized in the off-peak% range from 0% to 2%, while in the off-peak% range more than 2%, the quality of image becomes bad and the change in image is clearly visualized.

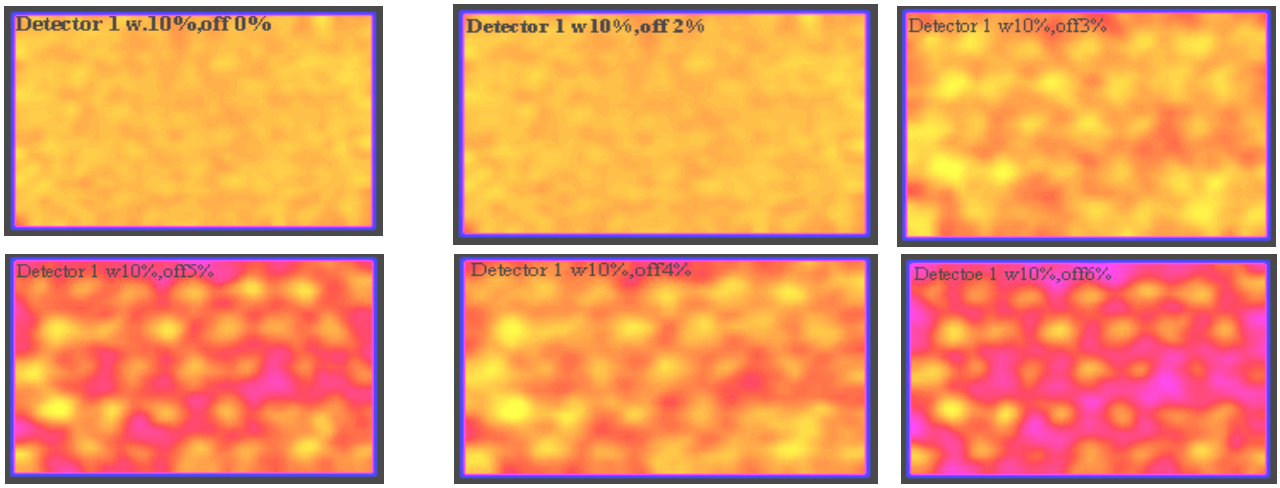

Fig. 5 represents the flood images for different off-peak percentage at window width of 10%.

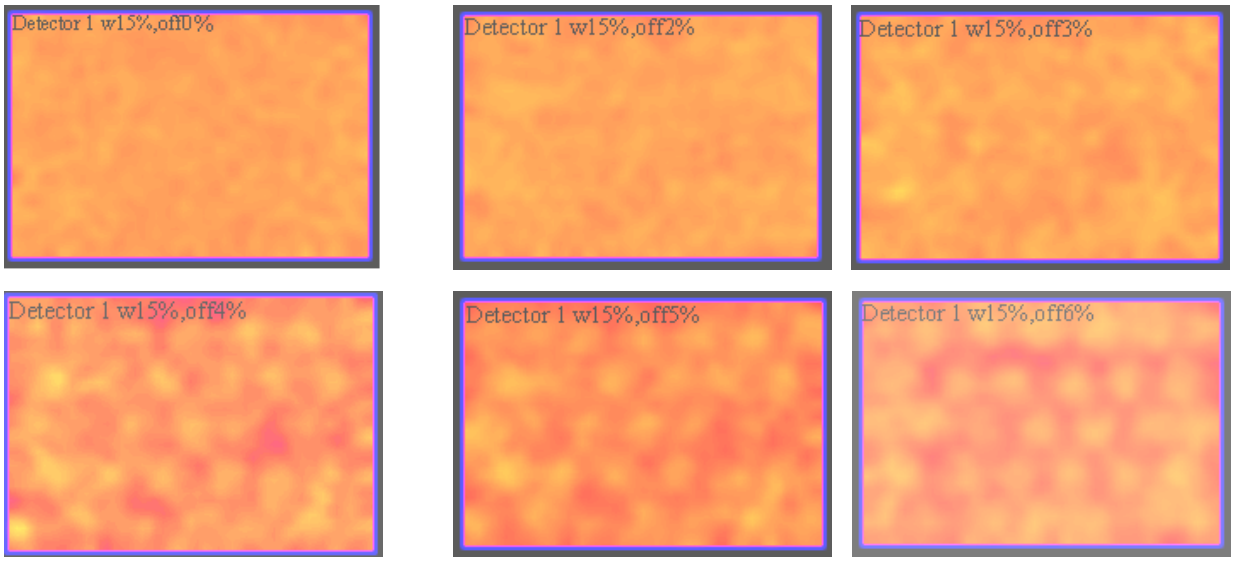

Fig. 6 represents the flood images for different off-peak percentage at window width of 15%.

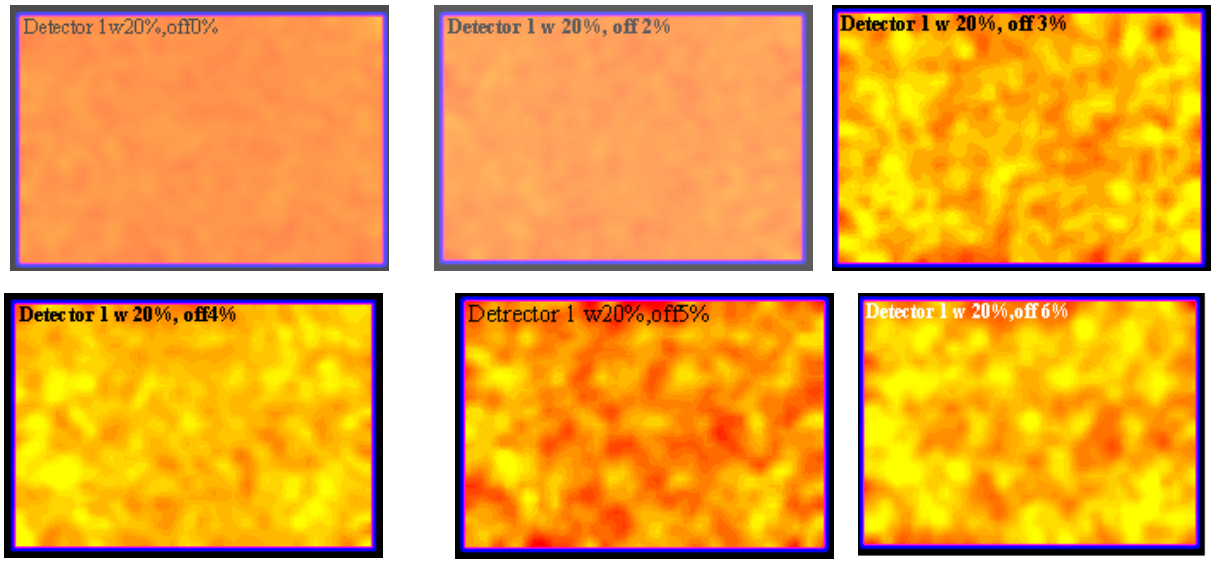

Fig. 7 represents the flood images for different off-peak percentage at window width of 20%.

Fig. 8 shows the calculated values for both integral and differential uniformity values in CFOV and UFOV versus the percentage of window width at off-peak shift of energy 0% shift. This figure shows a significant decrease in both the calculated integral and differential uniformity values in the range from 5% to 15% window width, indicating an increase in the image uniformity. While, in the range of window width from 15% to 25% a decrease in the image uniformity is observed, i.e., more increase in window width yields a significant loss in the image uniformity.

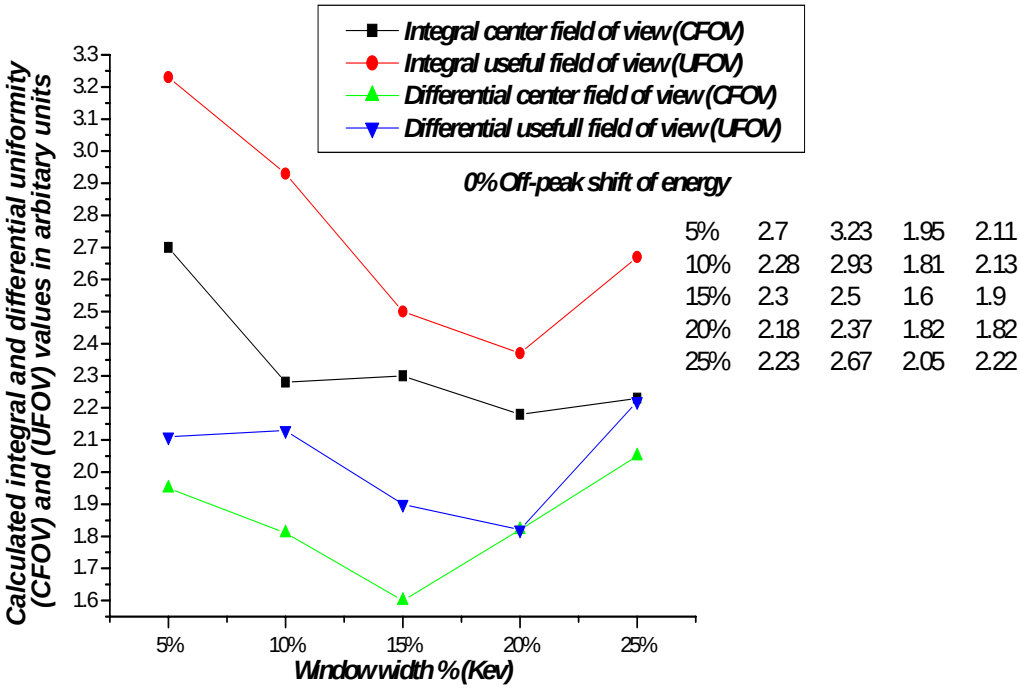

Fig. 8 represents the calculated integral and differential uniformity (CFOV) and (UFOV) values in arbitary units versus Window width% in KeV at 0% off-peak shift of energy.

Fig. 9 shows 4 images of thyroid scan taken for the same patient with different off-peak shifts 0%, 2%, 4% and 6%. A decrease in the overall activity with loss in image quality is observed. From the medical point of view, the first image indicates a normal and uniform tracer uptake pattern opposite both thyroid lobes with no focal lesions (i.e., normal morphology and function of the thyroid gland). In the second, third and forth images there are a decrease in the overall uptake in the salivary glands, thyroid gland and background, with no difference in sintigraphic diagnosis.

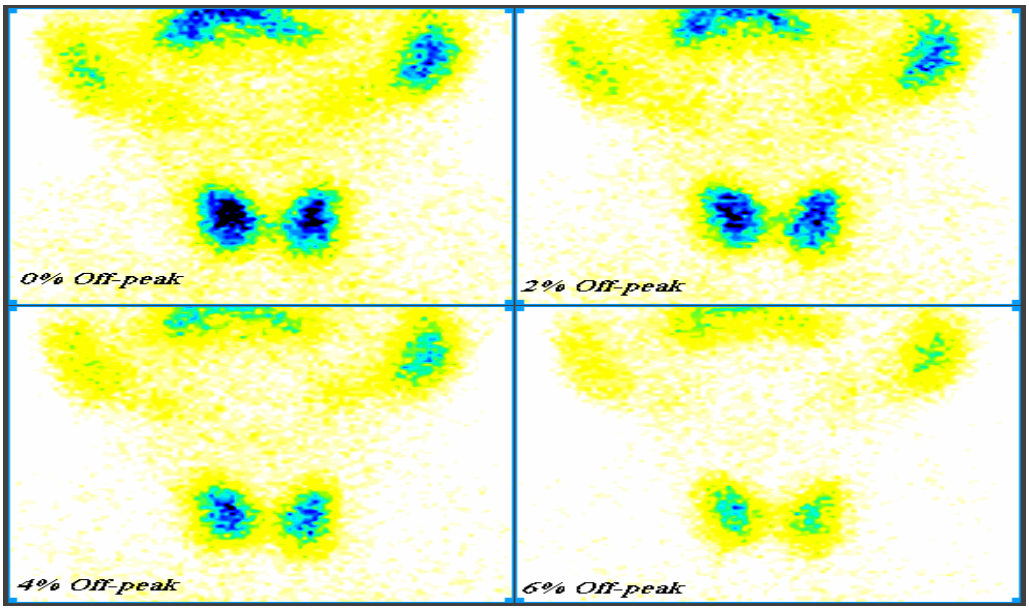

Fig. 9 Tc-99mThyroid scan (1) 0% off-peak (2) 2% off-peak (3) % off-peak (4) 6% off-peak.

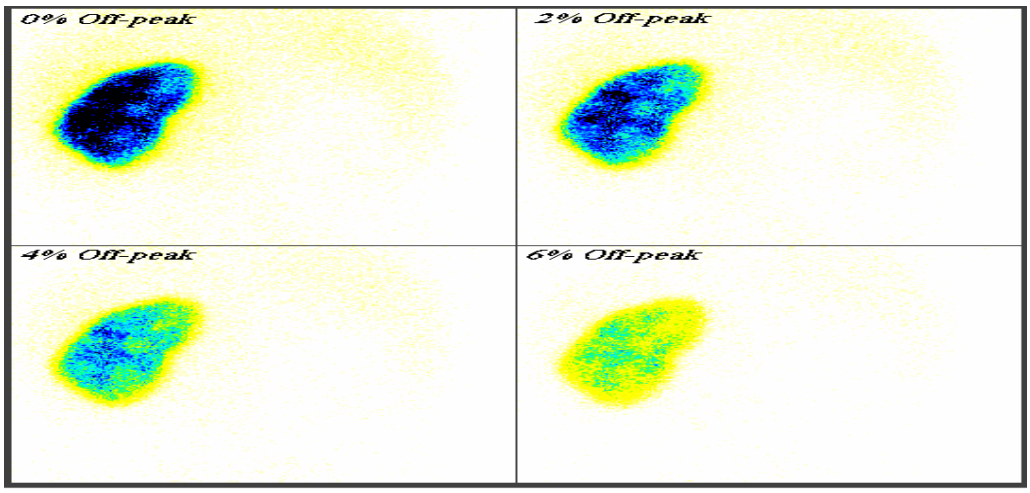

Fig. 10 Tc-99m renal scan (1) 0% off-peak (2) 2% off-peak (3) 4% off-peak (4) 6% off-peak.

Fig.10 shows 4 images of kidney scan taken for the same patient with different off-peak shifts 0%, 2%, 4% and 6%. Different quality of images is shown in the scan, which indicates a change in the tracer distribution of the kidney. From the medical point of view, the first image indicates a normal, good and uniform tracer uptake pattern with normal cortical portrayal; the second image shows a mild decrease in the overall tracer content which indicates an early diffuse parenchyma renal disease. The third image shows a moderate overall decrease in the tracer uptake with moderately decrease in the overall cortical tubular function. The fourth image shows a marked decrease in renal uptake with thin (atrophic) cortex, which can be attributed to chronic parenchyma renal disease with marked cortical tubular function loss.

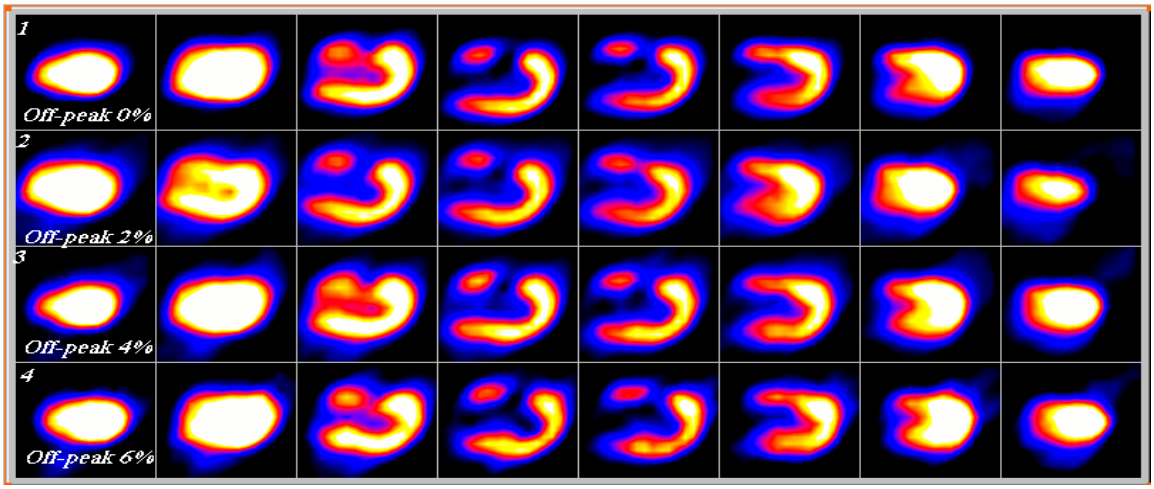

Fig. 11 heart phantom SPECT (1) off-peak 0% (2) off-peak 2% (3) off- peak 4% (4) off-peak 6% at window width 10%.

Fig. 11 shows 4 rows of vertical long axis cuts of heart phantom SPECT with 4 off-peak shifts at window width of 10%. This Fig. shows a loss in the recorded counts as seen in the rows from the upper one to the last one. This loss in the recorded counts may be due to off-peak shift, which may result in over estimating physician diagnostic. From the medical point of view, in the first to third rows there is a single moderate sized perfusion defect that shows marked hypoperfusion. Images in the forth row show degraded quality with

exaggerated defect (large area of sever hypoperfusion). In addition, the inferior wall shows rather non-uniform tracer distribution.

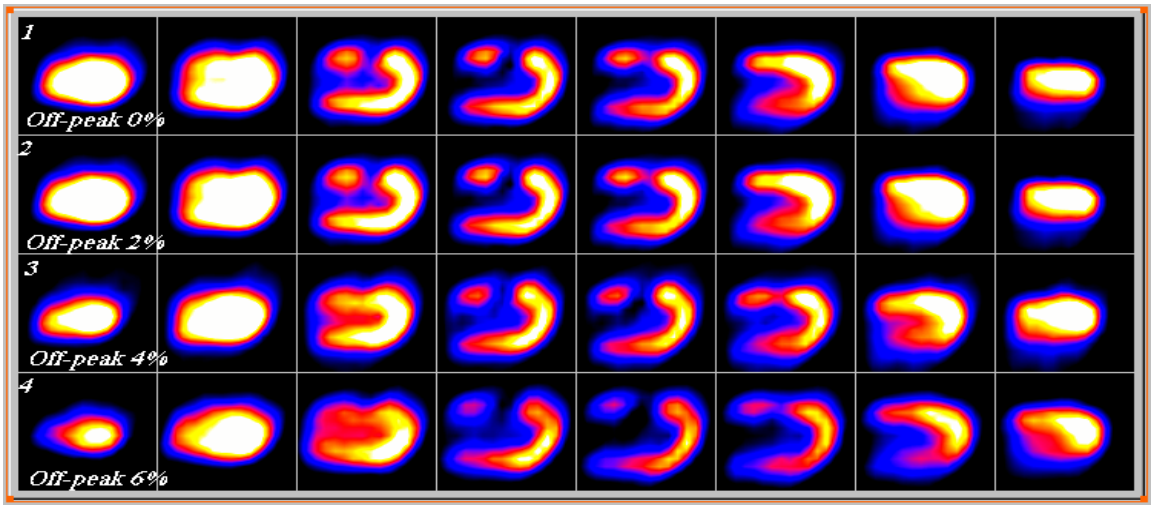

Fig. 12 heart phantom SPECT (1) off-peak 0% (2) off-peak 2% (3) off-peak 4% (4) Off-peak 6% at window width 15%

Fig. 12 shows 4 rows of vertical long axis cuts of heart phantom SPECT with 4 off-peak shifts at window width of 15%. Fig. 12 shows a loss in the recorded counts as seen in the rows from the upper one to the lower one. This loss in the recorded counts may be due to off-peak shift, which may result in over estimating physician diagnostic. From the medical point of view, in the first row there is a single defect in the anterior wall, otherwise normal myocardial perfusion pattern. In the second row, In addition to the previous effect, there is a mild hypoperfusion of the basal anterior wall. In the third row, In addition to the previous effects, there is a moderate hypoperfusion of the basal anterior wall and mild hypoperfusion of the inferior wall. In the fourth row, in addition to all previous effects, there is a marked hypoperfusion of the basal wall and moderate hypoperfusion of the anterior wall. From the medical point of view, all the previous effects result in an increase in size and degree of hypoperfusion of the true defect. This false perfusion defect appeared with enlarge size and severity in the anterior and inferior wall.

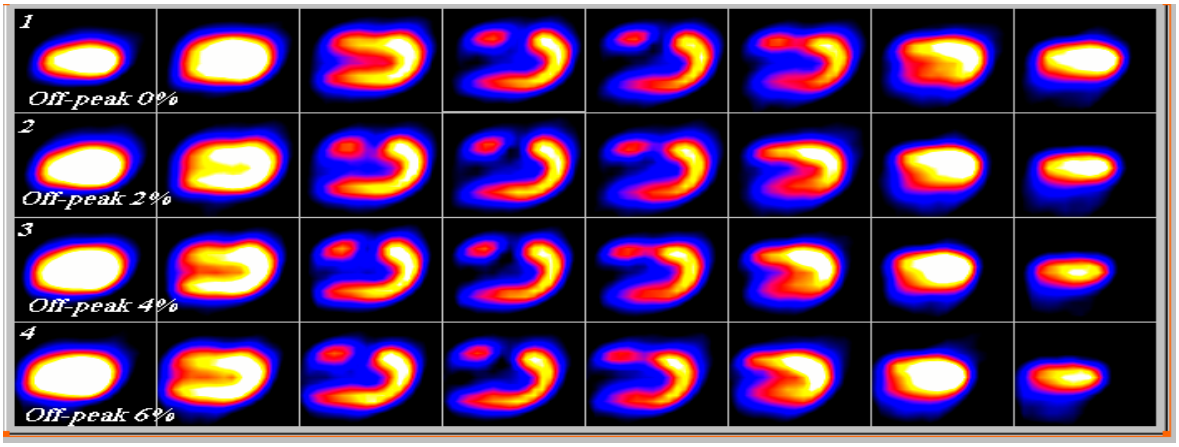

Fig. 13 heart phantom SPECT (1) off-peak 0% (2) off-peak 2% (3) off-peak 4% (4) Off-peak 6% at window width 20%

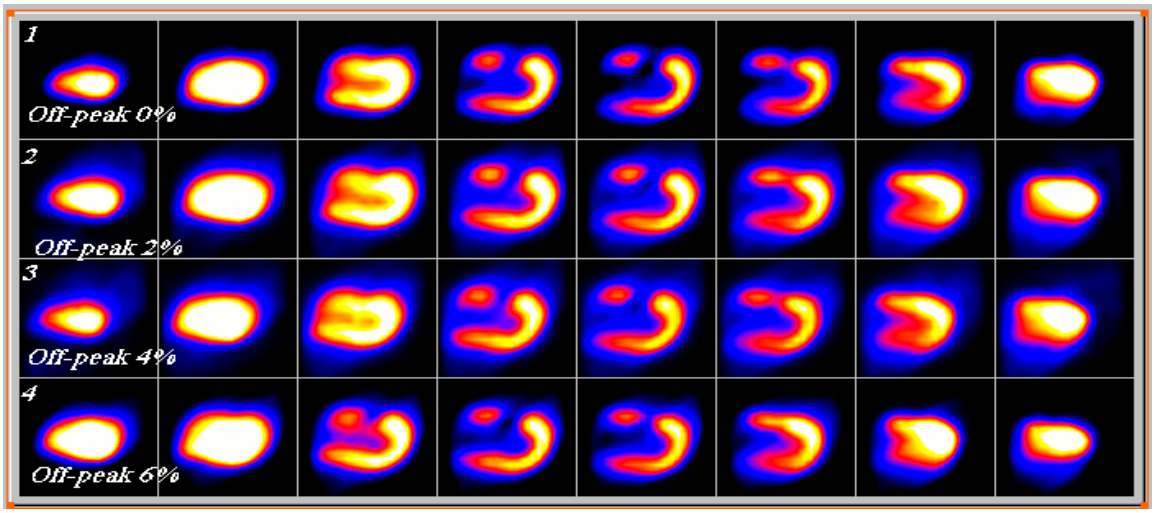

Fig. 14 heart phantom SPECT (1) off-peak 0% (2) off-peak 2% (3) off-peak 4% (4) Off-peak 6% at window width 25%

Fig. 14 shows 4 rows of vertical long axis cuts of heart phantom SPECT with 4 off-peak shifts at window width of 25%. Fig. 14 shows a loss in the recorded counts as seen in the rows from the upper one to the lower one. This loss in recorded counts may be due to off-peak shift, which may result in a bad estimating physician diagnostic.

Conclusion:

Gamma camera must work at some optimum conditions to avoid interpretation mistakes, which can be generated due to the protocol errors. In the present study, we investigated the effect of both of off-peak shift and window width shift of energy on planer and SPECT image uniformity using the calculated integral and differential center field of view (CFOV) and useful field of view (UFOV) uniformity values versus the change in both of off-peak and window width shift. We concluded that the optimum off-peak shift was 0% shift, but practically we can acquire data at 0% and 2% off-peak shifts without deeply effect on the image quality. The optimum window width shift was in the range from 15% to 20% shift of energy for the used radiopharmaceutical. In SPECT study, the effect of off-peak and window width shift applied on heart phantom affected the quality of images strongly leading to different clinical diagnosis, and the optimum window width shift was in the range from 15% to 20% of energy for the used radiopharmaceutical. Finally, a high level of severity with a false diagnosis have reported with the application of off-peak and widow width shift of energy on patients during the thyroid and kidney scan.

References:

1. Agostini ADe, Zatta G, Bagliani G, Tarolo GL: Proposal for a quality control procedure for rotating gamma camera tomographic systems. Radiol Med (Torino) :74 (1-2), 109-115, 1987.
2. Baron JM, Chouraqui P: Myocardial single-photon emission computed tomographic quality assurance. J Nucl Cordial: 3(2), 157-166, 1996.
3. De Puey EG: How to detect and avoid myocardial perfusion SPECT artifacts: J Nucl Med: 35(4), 699-702, 1994.
4.Early PJ: Text book of nuclear medicine technology: 4th add Mosby, 180-248, 1995.
5. Graham LS: Quality control for SPECT systems: Radiographic 15(6), 1471-1481, 1995.

6. Groch MW and Erwin WD: Single-Photon Emission Computed Tomography: Instrumentation and Quality Control. J.N.M. Technology, Volume 29, Number, 12-18., (2001).
7. Groch, M.W., and Erwin, W.D., Spect in year 2000: Basic principles. JNM Technology: 28, No.4, 233-244, 2000.
8. NEMA: performance measurements of scintillation cameras, standards publication no. 1. 1994.
9. O'Connor MK: Instrument- and computer-related problems and artifacts in nuclear medicine. Semin Nucl Med: 26 (4), 256- 277, 1996.
10. Saw CB: Effects of centre-of-rotation shift on contrast and spatial resolution of the SPECT system. Nucl Med Common: 7 (5), 373-379, 1986.
11. Sorenson JA, Phelps ME: Physics in nuclear medicine. 2nd edition, Grune and Stratton, Inc 298-302, 1987.
12. Spies SM: Oral Communications, an example of an initial bone scan using the Starbrite TM crystal system (Sept 2000).
13. Young KC, Kourisk, Awdeh M, Abdel-Dayem HM: Reproducibility and action levels for gamma camera uniformity. Nucl Med Commune: 11 (2), 95-101, 1990.